Deep CNN based droplet deposition segmentation for spray distribution assessment

Tao Chen
School of Computer Science and Electronic Engineering
University of Essex, Colchester, U.K.
tc17339@essex.ac.uk

Yanhua Meng
School of Mechanical Engineering,
Anyang Institute of Technology, Anyang, China
yanhua.meng@outlook.com

Jinya Su
Department of Computing Science
University of Aberdeen, Aberdeen, U.K.
jinya.su@abdn.ac.uk

Cunjia Liu
Department of Aeronautical and Automotive Engineering
Loughborough University, Loughborough, U.K.
C.Liu5@lboro.ac.uk

***Abstract*—Pesticides have been widely used in the cultivation of crops to enhance their production, however, incorrect application of pesticides will result in yield loss, product waste, environmental pollution among many others. Therefore, timely evaluating spray distribution of intelligent sprayers plays a pivotal role in the appropriate delivery of pesticides to the crop. The exiting approaches based on water-sensitive paper (WSP) either involve a relatively tedious and labor-intensive procedure, or have a high requirement on WSP image taking. So in this study we aim to conduct spray distribution assessment in the field based on mobile devices. To this end, the key issue of droplet deposition segmentation under natural imaging environments is addressed. WSPs with food dye droplets are first collected in the field by mobile phones. Then an image dataset on droplet deposition segmentation is created via thresholding approach with human supervision. Then four popular deep convolutional neural network (CNN) based segmentation algorithms are applied for droplet deposition segmentation so that spray distribution can be assessed. Comparative experiments show that UNeXt network is the best one in consideration of accuracy, inference time and network size.**

***Index Terms*—Convolutional neural network (CNN); Droplet segmentation; Pesticide spray analysis; Precision agriculture; Semantic segmentation; Water sensitive paper.**

I. Introduction

An increasing world population, projected to be 9 billion by 2050, is placing an unprecedented demand on agriculture, almost 70% more food demand increase. This global challenge is even severer by considering the scarcity of the arable land and natural resources, climate change and the societal demand for shrinking agriculture's environmental footprint for its sustainable development [1], [2]. Crops, however, are threatened by various stresses (e.g., abiotic stresses, pathogens and pests) in their life-cycle, which if managed inappropriately will lead to yield loss and quality degradation, posing serious threats on food security. In particular, it is estimated that about 30% of the crop loss worldwide is due to the adverse effects of weeds, diseases and insect pests annually [3]. Two approaches are generally available to attenuate the side effects of these issues including chemical control and genetic resistance [4].

Although there is much progress in genetic resistance, at present, chemical control, i.e., the application of pesticides is still the dominant approach (e.g. representing a $40 billion yearly budget) to enhance crop production, particularly in developing countries and regions [5]. In this context, it is significant that the right amount of pesticides should be sprayed on the target crop areas of interest. This is because, on the one hand, excessive uses of pesticides may leave residues in the agricultural products along with ecological tainting (e.g. increasing the likelihood of ground war contamination) and a high cost, generating significantly economical, environmental and social burdens [6]; on the other hand, insufficient doses of pesticides may result in areas of the harvest fields that are not protected, lessening crop productivity.

Therefore, it is highly desirable to develop an automated spray distribution assessment system so that spraying variables and parameters (e.g., nozzle type, droplet size, flow rate, operational parameters of spraying systems such as flight height and velocity in UAVs based sprayers) of agricultural sprayers can be evaluated and optimised in a short time window for a better spray distribution [3]. Various efforts have been made for this purpose in the past two decades including imaging and no-imaging based approaches. It is noted that only imaging based approaches are briefly introduced in this work due to the lack of space.

One notable work for this end is the DepositScan framework [7] proposed in 2011, which is made of the DepositScan software program and a handheld card scanner. In this framework, the WSPs are first collected, and scanned by the handheld business card scanner, which can obtain the image pixel information due to the fixed width of scanner and the scanner resolution (i.e., dots per inch or dpi). Then the scanned images can be analysed by the open-access ImageJ software

This work was supported by UK Science and Technology Facilities Council (STFC) under Newton fund with grant number ST/N006852/1 and ST/V00137X/1. Cunjia Liu is also supported by the Royal Society funding under the grant No. IEC\NSFC\191320. Yanhua Meng is also supported by the 2021 Anyang Science and Technology Project with project No. 2021C01NY037.

in the DepositScan program. As a result, different key metrics for spray distribution can thus be calculated including spray coverage, number of droplets in unit area and droplet size distribution. It is noted, however, that this scanning based framework is inconvenient for field applications due to the relative tedious and labor-intensive procedure therein.

Recent efforts have been made to develop field devices or applications for onsite spray distribution assessment instead of offline indoor processing. For example, [8] designs an intelligent vision sensor node for WSP image collection, which can adapt to the changes of light intensity in the environment. Then a watershed segmentation algorithm is applied to separate the droplets in the image. However, the system involves an elevated cost, constraining its wide adoptions.

Alternatively, there are also several smartphone based imaging approaches, which rely on smartphones for image collection and algorithm implementation. This approach is conceived to be promptly accessible, and portable to the fields. In this context, SnapCard [9] is the first pesticide spray coverage tool running on a smartphone, which only supports the coverage area of the WSPs. DropCard with DropScope is a commercial smartphone application which relies on an external water-card reader under restricted card sizes. In 2021, DropLeaf [5] is proposed, where image analysis pipeline is developed to analyze the WSP images taken carefully by the smartphone. The pros and cons of the three smartphone based applications for pesticide spray assessment are summarized in Table 1 of [5]. It should be noted that the state-of-the-art DropLeaf has a high requirement on WSP image taking.

Therefore, the main aim of the study is to develop a droplet deposition segmentation system so that images of WSPs taken in the field conditions by various mobile devices can be automatically segmented, so that the spray distribution of various sprayers can be evaluated quickly in the field conditions. To this end, WSPs are first collected at different locations of the citrus wogan structure and under different spraying parameter settings. Then images of the WSPs are taken in the field conditions by different mobile devices. Considering the high workload involved in manual droplet annotation, thresholding method is then used to segment the droplets from the WSP background for the purpose of image labelling, where the threshold is manually chosen by human experts. Suitable regions of interest of the segmented WSP images are chosen to construct the training image dataset. On this basis, various deep CNN based segmentation approaches are compared to identify the most suitable one for droplet deposition segmentation. Some spray distribution metrics can thus be calculated based on the segmented images. To be more exact, the main contributions are summarized as below.

1) *Dataset*: An image dataset for droplet deposition segmentation is generated by taking images of WSPs and labelling via manually choosing thresholds and region of interest (ROI) cropping.
2) *Algorithm*: Various deep CNN based segmentation algorithms are compared for droplet deposition segmentation with good performance.

II. Materials and Methods

In this section, materials and methods relevant to the study are introduced such as WSP image collection, image labelling and labelled dataset generation, droplet deposition segmentation and metric calculation for spray distribution assessment. To ease the understanding of this study, the flowchart of the developed framework is displayed in Fig 1.

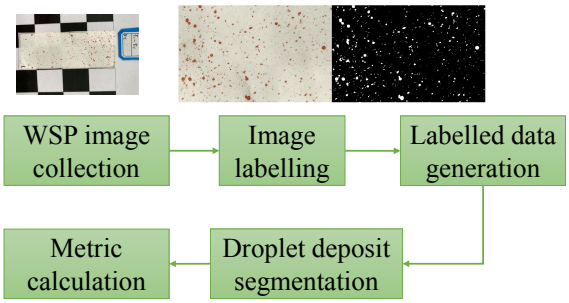

Figure 1. Flowchart of the developed framework including WSP image collection, image labelling, labelled dataset generation, droplet deposition segmentation and metric calculation for spray distribution.

A. WSP image collection

In the experiment, instead of directly spraying pesticide, red food dye is adopted due to its low price and color differences from the WSP background. WSPs are placed at three different positions of the citrus crop. At the same time, different operation parameters are adopted in the experiments so that different droplet distributions can be obtained.

Upon spraying droplets being collected by the WSPs, WSPs are placed above the printed reference calibration checkerboard, where the black and white squares have a fixed size of 1×1 cm. Then images are taken by different mobile phones under different illumination conditions, where the imaging rule is summarized as below: (1) the phone (with down-facing camera) is placed above the WSPs so that the WSPs are in the center of the image; (2) the phone is close enough to the WSPs to guarantee a high spatial resolution but meanwhile also make sure the images have no blur; (3) at least one white square should be visible in the image so that the pixel physical size can be determined. Some exemplary WSP images with different spray distributions are displayed in Fig. 2.

B. Methods

In recent years, image segmentation has been undergoing a significant progress, especially with the popularity of deep learning methods. In this study, we also aim to exploit deep CNN learning technique to segment the spraying droplets from WSP background. Deep learning methods, especially supervised deep learning methods, are generally data-hungry, and there is no such a dataset which focuses on droplet deposition segmentation. Hence, we create a dataset in which annotation is done by thresholding color images in Hue-Saturation-Value (HSV) color space. Image labelling and labelled dataset generation, droplet deposition segmentation

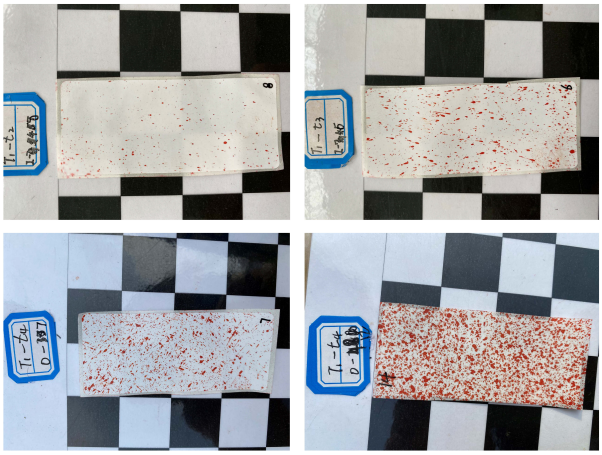

Figure 2. Exemplary WSP images with different spray distributions taken by different mobile phones under different illumination variations.

and metrics calculation for spray distribution assessment are detailed as below.

*1) **Image labelling and dataset generation**:* In order to build the deep CNN based droplet deposition segmentation model, a labelled dataset should be first generated for this supervision learning task. Considering the high workload in manually labelling the droplets one by one in WSPs, an image labelling algorithm in Algorithm 1 is proposed.

In this approach, a suitable grayscale image is first obtained by the RGB color bands or color space transformation (e.g. HSV) of the original RGB image or different vegetation indices [10]. Then the thresholding approach is adopted for the grayscale images, where the threshold is manually chosen for each sample WSP so that the labelling errors can be minimized. In addition, due to the substantial illumination changes in practical field conditions, the thresholding approach may be only valid for some part of the WSPs even various thresholds are chosen for different WSPs. So the correctly segmented regions are cropped out by abandoning the wrongly segmented areas.

Until this step, we already have the dataset and its labels for training a deep network, but the images so far have various image sizes (e.g. length and width), which is unable to feed to different deep networks for a fair comparison. Therefore, after image labelling, we further process the images to a fixed image size, which is 128×128 pixels in our setup. In particular, given a labelled image, a sliding window of size of 128×128 starts from the top-left corner of the image and crop the corresponding regions of size 128×128. Meanwhile, the corresponding label images are also cropped in the same way as its original label images so that image pairs are generated including source image and label image. Then the sliding window is moved with the stride of 10×10 pixels in width and height directions until it reaches the bottom-right corner of the image. To this end, our dataset consists of 3600 images where 80% are used for training, 10% for validation and the remaining 10% for testing. In Fig. 3, four selected exemplary images and their labels are shown. Note that these images are taken under various lighting conditions.

Algorithm 1 Semi-automatic labelling for dataset generation

Input: WSP images.
Output: Labelled dataset for model construction.
Step 1: Do RGB band separation or color space transformation (e.g. HSV) to obtain a suitable grayscale image;
Step 2: Separate the droplet depositions from the background via thresholding approach with manually chosen threshold for each WSP;
Step 3: Crop the regions with good droplet segmentation performance by visual inspection;
Step 4: Construct the labelled dataset by generating a large number of image patches with a fixed size of 128×128 from the images in Step 3.

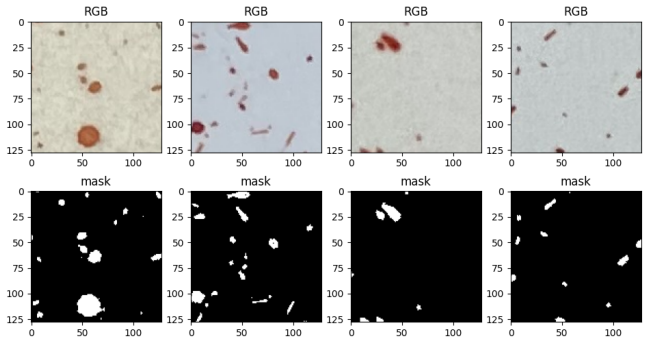

Figure 3. Exemplary image pairs including source RGB image (first row) and label image (second row) from our created dataset.

*2) **Droplet segmentation**:* Upon generating the labelled dataset for algorithm construction, we now consider the problem of droplet segmentation. In order to identify the most suitable model for droplet segmentation, we evaluate four state-of-the-art semantic segmentation networks including VGG16 [11], VGG16+CBAM (Convolutional Block Attention Module) [12], Unet [13], [14] and UNeXt [15] on our dataset.

Specifically, UNet and UNeXt are particularly-designed networks for medical images segmentation by using a few annotated data. In addition, VGG network is a well-known architecture and has shown significant performance in many computer vision tasks. In this study, we also explore the combination of VGG and an attention network CBAM to improve the representation of the features. The CBAM module is used to enhance the feature representation using two attention networks in channel and spatial axis, respectively.We insert the CBAM module into the second last layer of VGG16. The dimension of the features remain the same before and after the addition of the CBAM module. In order to obtain the droplet segmentation results, we modify the last layers of the aforementioned four networks, letting them generate two feature maps including background and foreground with the same size of input image. Their qualitative and quantitative comparison results will be analysed in section III.

Performance evaluation: To evaluate the performance of segmentation networks, we use metrics including Recall, Precision, F1-Score, Average precision score (AP), and Intersection over Union (IOU), where a higher value indicates better performance. In particular, the Recall and Precision are defined as below:

$$Recall = \frac{T_p}{T_p + F_n}, Precision = \frac{T_p}{T_p + F_p} \tag{1}$$

where T_p represents the number of true positive, F_n means the number of false negative, and F_p is the number of false positive.

F1-score, the harmonic mean of precision and recall, is able to consider recall and precision simultaneously. It is useful for imbalanced dataset and is calculated as:

$$F_1 score = 2 \times \frac{Precision \times Recall}{Precision + Recall}. \tag{2}$$

AP summarizes a precision-recall curve as the weighted mean of precisions achieved at each threshold, with the increase in recall from the previous threshold used as the weight. AP is defined as below

$$AP = \sum_n (Recall_n - Recall_{n-1}) \times Precision_n, \tag{3}$$

where $Precision_n$ and $Recall_n$ are the precision and recall at the n^{th} threshold.

IOU is the ratio of area of overlap/intersection over area of union, where a value closer to 1 means better performance.

$$IOU = \frac{Area\ of\ Overlap}{Area\ of\ Union}. \tag{4}$$

3) ***Metrics for spray distribution****:* After droplet segmentation, the next step would be computing the metrics evaluating the spray performance. There are generally three metrics quantifying the spray distribution including spray coverage (SP), number of droplets per unit area (NDUA, $droplets/cm^2$), droplet diameter distribution. In particular, SP refers to the relative zone occupied by the droplets in the Region Of Interest (ROI), which is calculated as below Eq. 5

$$SP = \frac{NoPixel\ by\ droplets}{NoPixel\ in\ ROI} \tag{5}$$

where $NoPixel_i$ denotes the No. of pixels.

Droplet diameter distribution is usually quantified by $D_{V0.1}$, $D_{V0.5}$, $D_{V0.9}$, which represent the distribution of the droplet diameters such that droplets with a diameter smaller than $D_{V0.1}$, $D_{V0.5}$, $D_{V0.9}$ compose 10%, 50% and 90% of the total liquid volume, respectively [7]. It is noted that in the calculation of the above metrics (except SP), the pixel resolution (e.g., the physical size of each pixel in the image) is vital, which is detailed as below.

In image analysis, the $Area_i$ of the i^{th} droplet can be calculated by the number of pixels occupied by the droplet multiplying the physical (instead of pixel) area of each pixel, which is given by

$$Area_i = NoPixel_i \times width_{px}^2. \tag{6}$$

where $NoPixel_i$ denotes the No. of pixels occupied by the i^{th} droplet, and $width_{px}$ refers to the physical size of each pixels (usually in the unit of μm), which can be calculated from the reference calibration checkerboard as below.

$$width_{px} = \sqrt{\frac{Area_{ws}}{NoPixel_{ws}}}. \tag{7}$$

where the $Area_{ws}$ denotes the physical area of the black/white square in the reference checkerboard (a known constant via its fixed size) and $NoPixel_{ws}$ refer to the No. of pixels occupied by one black/white square in the reference checkerboard. The detection of black/white squares for the $width_{px}$ will be implemented in the future.

Upon calculating the $Area_i$ of the i^{th} droplet, the droplet diameter of the i^{th} droplet can be derived from the formula of the circle area $Area_{circle} = \pi \times (\frac{diameter}{2})^2$, given by

$$Diameter_i = 2 \times \sqrt{\frac{Area_i}{\pi}}. \tag{8}$$

Then the calculation of $D_{V0.1}$, $D_{V0.5}$, $D_{V0.9}$ is followed by statically analysing the diameters of all droplets. It is noted that alternative/modified formula is also available in [7].

Finally, the calculation of NDUA is given as below

$$NDUA = \frac{No.\ of\ droplets}{Area_{ROI}}. \tag{9}$$

where $Area_{ROI}$ denotes the area of ROI and the No. of droplets in a ROI can be automatically obtained by applying image analysis function on the droplet segmentation images.

III. Results

This section presents the results including training details, test performance of different segmentation networks and spray coverage calculation.

A. *Training details*

The four networks are trained with a batch size of 16 and 200 iterations. The Adam optimiser is used for optimising VGG and VGG+CBAM with learning rate 1*e*-4. For the training of Unet and Unext, their hyperparameters are identical as in [13] and [15]. The networks are tested on a Nvidia GTX 1080 Ti graphic card. The loss function used for training is semantic cross-entropy loss, and it takes approximately 5 hours to converge.

B. *Droplet segmentation performance*

In Table I, we present the evaluation results of four networks on testing set. As one can see, all selected networks can achieve an F1 score of more than 80%, showing a relatively good performance.

Inference time: In Table II, we also list the time of networks for processing one image in the feed-forward calculation. The VGG network has the lowest inference time: 6.6 milliseconds per image. The lapsed time between mentioned networks is short and therefore it can be used for real-life applications.

Network Parameters: The size of network is a key index when deploying in practical applications, particularly, using

deep CNN in embedded system. Furthermore, considering the analysis to be done in the smartphone or other portable devices instead of workstation, we need a light-weight model for this task. In the second row of table II, we summarize the parameters of the aforementioned network. Both VGG and Unet networks have encoder-decoder like architecture, but Unet utilises the skip-connection, which can bring up global and local features to decoder part to construct more accurate performance. CBAM is a light-weight attention module, combing with VGG increases 24MB parameters compared with VGG only.

Table I
QUANTITATIVE EVALUATION RESULTS OF FOUR CNNS

	F1	*Precision*	*Recall*	*AP*	*IOU*
VGG	0.817	0.739	0.93	0.817	0.695
VGG+CBAM	0.845	0.779	0.933	0.848	0.736
Unet	0.884	0.838	**0.958**	**0.873**	0.799
UNeXt	**0.903**	**0.947**	0.869	**0.873**	**0.824**

Table II
INFERENCE TIME AND NETWORK SIZE

	VGG	VGG+CBAM	Unet	UNeXt
Time (second per frame)	0.0066	0.0068	0.0073	0.007
Total size (MB)	225.01	249.39	268.26	6.49

It is shown from Table. I and II that UNeXt network obtains the best performance in consideration of F1 score, Precision, Recall, AP, IOU, computation time and total size and so should be adopted in practical applications. This is mainly due to its improved design of network architecture, where convolutional networks are only used for learning low-dimensional features in early stage and tokenized Multi-layer perception (MLPs) to represent high-dimensional features by using few parameters compared with Convolutional network. Especially, this design demonstrates the ability to represent local dependencies that result in better segmentation performance in our test dataset.

Segmentation visualization: In Fig. 4, we present the qualitative segmentation results of the four CNNs, where the segmentation results of VGG, VGG+CBAM, Unet, and Unext are from second column to last column. There are five exemplary images with various illumination and spraying distributions chosen from our testing set. From the second column, VGG assigns some pixels to the background (smaller black holes in the white areas) which are false negative. These wrongly assigned pixels are mainly located in the spraying areas with unequally red color. With the auxiliary of CBAM, these false negative pixels have reduced slightly. From fourth column, we find that Unet can handle this problem better. But in the extremely case like the fifth source image, it encounters large areas of blurry droplets, VGG, VGG+CBAM, and Unet can not overcome this issue properly. In the contrast, Unext can still recognise these pixels as droplets.

C. Spray coverage calculation

In this subsection, we report the SP index of WSPs based on the segmentation result of Unext. The whole process of SP calculation is illustrated in Fig. 5. In step 1, we manually crop the WSP from the background as the physical size of pixel is not required in SP calculation. It should be noted that the cropped images have different image sizes from the training samples and can not be directly feed to Unext. So in step 2, we resize the images to a larger square size 1024×1024 so that Unext can process them. In step 3, the fixed-size images are provided to Unext to obtain the masks of droplet. In SP calculation, the masks (white pixels) are treated as the droplet and the whole images are treated as the ROI. In the end, the spray distribution can simply be calculated via Eq. 5, which are 5.7% and 38.1% for WSP1 and WSP2, respectively.

IV. CONCLUSIONS AND FUTURE WORK

This work considers the challenges of spray distribution assessment via water sensitive paper images taken in field conditions. The main task under investigation is first transformed into droplet deposition segmentation under illumination changes, where droplets are labelled in a semi-automatic manner via manually tuned thresholds. Then four popular deep convolutional neural networks (CNNs) including VGG, VGG+CBAM, Unet and UNeXt are compared to identify the most suitable one for droplet deposition segmentation task. It is shown that UNeXt is the best one in consideration of accuracy performance, inference time and network size.

Although the performance of droplet deposition segmentation is satisfying and some metrics quantifying spraying distribution (e.g. spray coverage) are also obtained, there is still much room for further development in order that the developed system can be applied in real-life application for in-field spray distribution assessment. These aspects are summarized as below.

1) The dataset can be expanded to include more real-world field imaging conditions so that the semantic segmentation models become more robust and reliable.
2) More spraying distribution metrics (e.g. droplet number in unit area, droplet diameter distribution) can be calculated with the advert of pixel size information obtained from the reference checkerboard, and compared against the ground truth metrics obtained by the widely accepted approaches (e.g. Deposit Scan).
3) It would be interesting to see whether the developed framework can be translated to directly evaluating spraying distribution on crop leaves instead of water sensitive papers by using food dye of suitable concentration.

REFERENCES

[1] J. A. Foley, N. Ramankutty, K. A. Brauman, E. S. Cassidy, J. S. Gerber, M. Johnston, N. D. Mueller, C. O'Connell, D. K. Ray, P. C. West, *et al.*, "Solutions for a cultivated planet," *Nature*, vol. 478, no. 7369, pp. 337–342, 2011.

[2] J. Su, D. Yi, M. Coombes, C. Liu, X. Zhai, K. McDonald-Maier, and W.-H. Chen, "Spectral analysis and mapping of blackgrass weed by leveraging machine learning and uav multispectral imagery," *Computers and Electronics in Agriculture*, vol. 192, p. 106621, 2022.

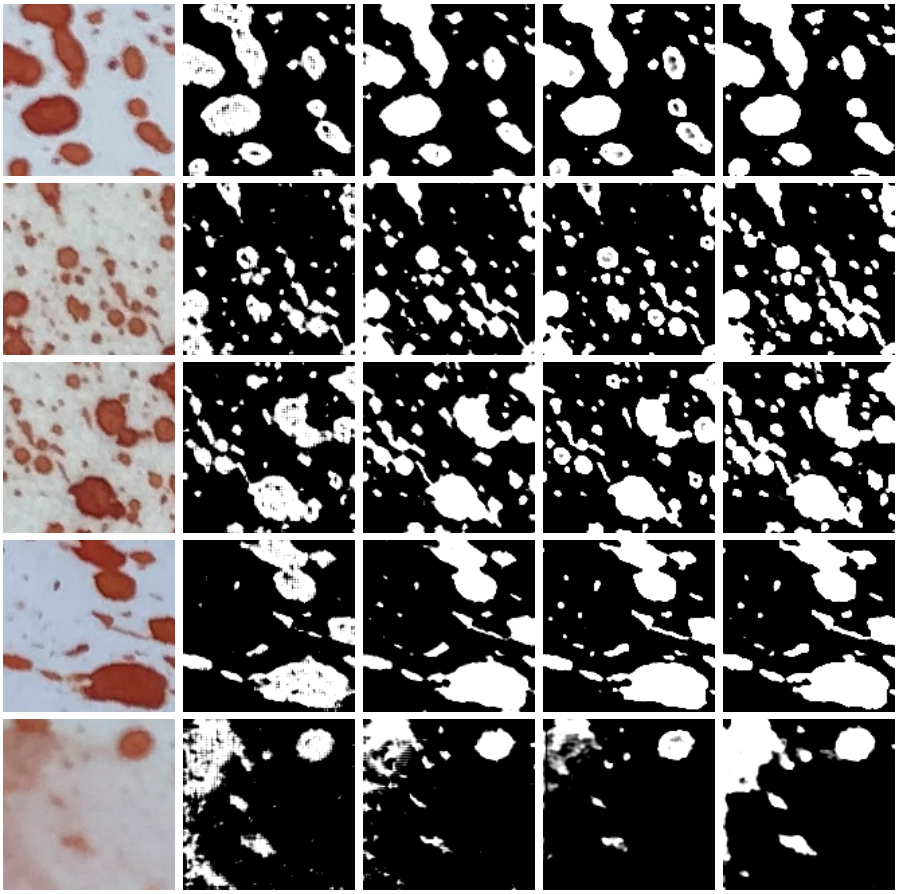

Figure 4. Exemplary segmentation results: from left to right, RGB source image, VGG, VGG+CBAM, Unet, Unext.

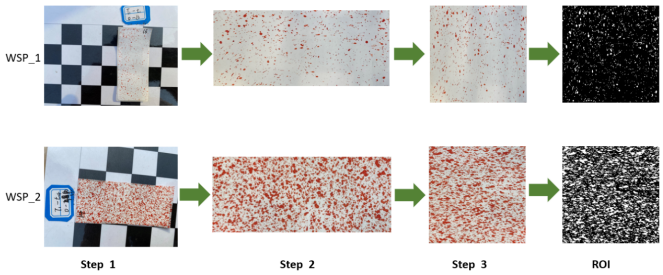

Figure 5. Procedures of obtaining ROIs

[3] Y. Meng, J. Su, J. Song, W.-H. Chen, and Y. Lan, "Experimental evaluation of uav spraying for peach trees of different shapes: Effects of operational parameters on droplet distribution," *Computers and Electronics in Agriculture*, vol. 170, p. 105282, 2020.

[4] Z. Mi, X. Zhang, J. Su, D. Han, and B. Su, "Wheat stripe rust grading by deep learning with attention mechanism and images from mobile devices," *Frontiers in Plant Science*, p. 1386, 2020.

[5] B. Brandoli, G. Spadon, T. Esau, P. Hennessy, A. C. Carvalho, S. Amer-Yahia, and J. F. Rodrigues-Jr, "Dropleaf: A precision farming smartphone tool for real-time quantification of pesticide application coverage," *Computers and Electronics in Agriculture*, vol. 180, p. 105906, 2021.

[6] W. Farha, A. Abd El-Aty, M. M. Rahman, J. H. Jeong, H.-C. Shin, J. Wang, S. S. Shin, and J.-H. Shim, "Analytical approach, dissipation pattern and risk assessment of pesticide residue in green leafy vegetables: A comprehensive review," *Biomedical Chromatography*, vol. 32, no. 1, p. e4134, 2018.

[7] H. Zhu, M. Salyani, and R. D. Fox, "A portable scanning system for evaluation of spray deposit distribution," *Computers and Electronics in Agriculture*, vol. 76, no. 1, pp. 38–43, 2011.

[8] L. Wang, X. Yue, Y. Liu, J. Wang, and H. Wang, "An intelligent vision based sensing approach for spraying droplets deposition detection," *Sensors*, vol. 19, no. 4, p. 933, 2019.

[9] C. Nansen, J. C. Ferguson, J. Moore, L. Groves, R. Emery, N. Garel, and A. Hewitt, "Optimizing pesticide spray coverage using a novel web and smartphone tool, snapcard," *Agronomy for Sustainable Development*, vol. 35, no. 3, pp. 1075–1085, 2015.

[10] J. Su, C. Liu, M. Coombes, X. Hu, C. Wang, X. Xu, Q. Li, L. Guo, and W.-H. Chen, "Wheat yellow rust monitoring by learning from multispectral uav aerial imagery," *Computers and electronics in agriculture*, vol. 155, pp. 157–166, 2018.

[11] K. Simonyan and A. Zisserman, "Very deep convolutional networks for large-scale image recognition," *arXiv preprint arXiv:1409.1556*, 2014.

[12] S. Woo, J. Park, J.-Y. Lee, and I. S. Kweon, "Cbam: Convolutional block attention module," in *Proceedings of the European conference on computer vision (ECCV)*, pp. 3–19, 2018.

[13] O. Ronneberger, P. Fischer, and T. Brox, "U-net: Convolutional networks for biomedical image segmentation," in *International Conference on Medical image computing and computer-assisted intervention*, pp. 234–241, Springer, 2015.

[14] J. Su, D. Yi, B. Su, Z. Mi, C. Liu, X. Hu, X. Xu, L. Guo, and W.-H. Chen, "Aerial visual perception in smart farming: Field study of wheat yellow rust monitoring," *IEEE transactions on industrial informatics*, vol. 17, no. 3, pp. 2242–2249, 2021.

[15] J. M. J. Valanarasu and V. M. Patel, "Unext: Mlp-based rapid medical image segmentation network," *arXiv preprint arXiv:2203.04967*, 2022.